Structural Monitoring and Maintenance, *Vol. 10, No. 3 (2023) 261-281*
https://doi.org/10.12989/smm.2023.10.3.261

Force monitoring of Galfan cables in a long-span cable-truss string-support system based on the magnetic flux method

Yuxin Zhang*[1], Xiang Tian[1], Juwei Xia[2] and Hexin Zhang[3]

[1]*School of Civil Engineering, Shanghai Normal University, Shanghai 201418, China*
[2]*Space Structures Research Center, Zhejiang University, Hangzhou 310027, China*
[3]*School of Computing, Engineering and the Built Environment, Edinburgh Napier University, Edinburgh EH10 5DT, Scotland, UK*

(*Received September 12, 2023, Revised September 17, 2023, Accepted September 20, 2023*)

Abstract. Magnetic flux sensors are commonly used in monitoring the cable force, but the application of the sensors in large diameter non-closed Galfan cables, as those adopted in Yueqing Gymnasium which is located in Yueqing City, Zhejiang Province, China and is the largest span hybrid space structure in the world, is seldom done in engineering. Based on the construction of Yueqing Gymnasium, this paper studies the cable tension monitoring using the magnetic flux method across two stages, namely, the pre-calibration stage before the cable leaves the rigging factory and the field tension formation stage of the cable system. In the pre-calibration stage in the cable factory, a series of 1:1 full-scale comparative tests were carried out to study the feasibility and relability of this kind of monitoring method, and the influence on the monitoring results of charging and discharging voltage, sensor location, cable diameter and fitting method were also studied. Some meaningful conclusions were obtained. On this basis, the real-time cable tension monitoring system of the structure based on the magnetic flux method is established. During the construction process, the monitoring results of the cables are in good agreement with the data of the on-site pressure gauge. The work of this paper will provide a useful reference for cable force monitoring in the construction process of long-span spatial structures.

Keywords: cable tension monitoring; cable-truss string-support system; Galfan cable; long-span spatial structures; magnetic flux sensor

1. Introduction

Cable structures are widely used in long-span spatial structures, long-span bridges, and other projects. A cable-truss system is one of the most active structural forms in the field of space structures to achieve a large span. In recent years, it has been widely used in the World Cup and Olympic stadiums, such as Busan Stadium in Korea by Eul and Seok (2008), Maracana Stadium in Brazil by Wolfgang (2014) and so on.

*Corresponding author, Professor, E-mail: zyx@shnu.edu.cn
[a]Graduate Student, E-mail: 17860732171@163.com
[b]Ph.D. Student, E-mail: gdshx2006@163.com
[c]Associate Professor, E-mail: j.zhang@napier.ac.uk

Copyright © 2023 Techno-Press, Ltd.
http://www.techno-press.org/?journal=smm&subpage=7 ISSN: 2288-6605 (Print), 2288-6613 (Online)

Ding *et al*. (2014) summarized the structural forms of this new cable-truss system and introduced its potential engineering applications. At present, most cable truss systems are built using closed ring cable structures covered with flexible membrane roofs. Summarizing typical engineering case studies across the world, the structure exhibits a beautiful form and performs reasonably in terms of stress (Mike 2012, Coarita and Flores 2015, Zurru 2021). The roof structure of Yueqing Stadium breaks through the constraint of closed ring cables and adopts the non-closed crescent-shaped cable-truss system (Li *et al.* 2015). Yueqing Gymnasium further surpasses the limitation of hollow ring cables and flexible membrane roofs, adopting the roof structure of a cable truss system to completely close and cover the rigid roof, as shown in Fig. 1. The roof structure is composed of both a rigid and flexible system, as shown in Fig. 2. The lower cables of the cable truss system are a free-form shell while the upper cables pass through the roof, the upper and lower cables then form a space bearing system with large equivalent thickness through slings, compression bars and ring cables. It has the characteristics of both cable truss and string support systems and can be called a cable-truss string-support structure. The cable-truss string-support structure system is similar to the cable supported system. The main cable system includes radial diagonal cables, compression bars and ring cables. However, the upper and lower cables are connected by slings and compression bars, and only the innermost compression bar is connected with the ring cables, thus it is a new hybrid space structure system with the characteristics of a cable truss system (Li *et al.* 2017). In addition to this hybrid system, the Yueqing Gymnasium project uses large-diameter non-closed Galfan cables.

The tension of the cable is an important structural component of the cable-truss string-support structure, and whether it reaches the expected design value is of great importance in structural design (Jakiel and Manko 2017). If the cable tension cannot meet the design requirements, the safety of the structure will be affected, and there will be instability or changes in the geometric composition of the system in serious cases. Due to several factors such as construction errors, environmental conditions, relaxation, etc., the cable force often changes. Therefore, it is necessary to frequently monitor the cable force to avoid disasters in time and for some large-span projects with cables this monitoring occurs during the construction period or service period (Gaute *et al*. 2022, Kim 2014).

At present, the commonly used cable force identification methods mainly include the pressure gauge method, anchorage cable force meter method, vibration method (Azim *et al*. 2020, Geuzaine *et al.* 2021, Timothy *et al.* 2018, Kim and Park 2007, Guido *et al.* 2018, Furukawa *et al.* 2022, Acampora *et al*. 2014), and magnetic flux method (Camassa *et al.* 2021, Yu *et al.* 2021, Seunghee *et al.* 2014, Gordon *et al*. 2010, Hee *et al.* 2012). Among them, the magnetic flux method is one of the most commonly used for cable tension monitoring, so it is also called cable tension sensor. The magnetic flux sensor is made based on the magnetoelastic effect principle: when a ferromagnetic material (cable) is subjected to an external load, its internal mechanical strain/stress is generated, which correspondingly causes the change in its internal magnetization (permeability), i.e., the magnetoelastic effect (Xiong *et al.* 2012). The relationship between the change of magnetic permeability and the stress is established and the stress of the ferromagnetic material is finally determined. The magnetic flux cable tension measurement system includes two stages, namely the calibration stage and the actual measurement stage. Due to different cable types, sizes and other parameters, the magnetic permeability-cable force correlation varies between different cables. The cable structure should be calibrated one by one before leaving the factory to obtain the zero point of magnetic flux and calibrate the magnetic permeability-cable force correlation before practical engineering applications (Lin *et al.* 2017).

Because the magnetic flux method has the advantages of strong anti-interference ability, high measurement accuracy and long service life in cable monitoring, this technology is relatively mature

in conventional cable structures such as steel strands and parallel steel wire cables (Yuan and Wu 2011, Dong 2020, Zhou *et al.* 2019, Seunghee *et al*. 2012). Galfan cables (Galfan, 95% zinc-5% aluminum-mixed rare earth alloy coated cables) (Wang *et al*. 2018) are a new type of prestressed cable, the cable body itself has a certain metallic luster, which is integrated with the building structure, and has the advantages of beautiful appearance, strong corrosion resistance, good fire resistance, no rotation, and large friction factor (Barnard and Brown 2008, Liu *et al*. 2021, Sun *et al.* 2021). The surface of the cable body is not covered with PE, eliminating the PE stripping and protection processes in the construction process. Also, without secondary anti-corrosion treatment, it can complete the connection of the complex space structure through cable clamp bifurcation technology, which greatly improves the construction efficiency (Sun *et al.* 2019, Zhang *et al.* 2022, Sun *et al.* 2020), so it is favored by modern architectural designers. With the large-scale of buildings, the specifications of Galfan cables are also increasing.

The Yueqing Gymnasium project adopts non-closed Galfan cable and the magnetic flux method was adopted to conduct cable monitoring during the construction period. The application and research of this method with Galfan cables is still limited, and the following questions are raised: what is the cable monitoring effect when the magnetic flux sensor is applied to this new cable? Especially for large diameter Galfan cables (more than 100 mm), what is the monitoring effect? What is the effect of cable force monitoring when applied to the practical construction process of the new structural forms of large span cable-truss string-support system of Yueqing Gymnasium?

Based on the Yueqing Gymnasium project, this paper studies the magnetic flux cable monitoring problem of the large-span cable-truss string-support system in two stages, namely the calibration stage before the cable leaves the factory, the on-site cable tensioning construction stage. In the calibration stage at the cable factory, a series of 1:1 full-length comparative experimental studies were carried out, the feasibility of the magnetic flux method for monitoring such cable force was studied, and the influence of charging and discharging voltage, cable length, sensor position, cable diameter and fitting method on the monitoring results were studied. Some important conclusions were obtained. On this basis, the real-time cable monitoring system using the magnetic flux method during the tensioning construction process is established. By analyzing the results of the cable monitoring system in the tensioning construction stage, it was found that the EM sensor can effectively reflect the pre-tension change of the structural tensioning construction stage, and this work will provide a useful reference for the cable force monitoring of large span spatial structures.

2. Project overview

Yueqing Gymnasium is located in Yueqing City, Zhejiang Province, China, and it is a 6000-seat gymnasium with a construction area of 21,796 m^2. The roof structure of the stadium has a simple and novel form which adopts a long-span cable-truss string-support system composed of a flexible radial cable truss system and a rigid single-layer free-form shell. The plane projection shape of the roof structure is an ellipse with a major axis of 148 m and a minor axis of 128 m, which is currently the hybrid space structure with the largest span in the world, as shown in Fig. 1.

Yueqing Gymnasium breaks through the limitation of hollow ring cables and a flexible membrane roof, and the roof structure using a cable truss system is completely closed and covered with a rigid roof. The roof structure is composed of both a rigid and flexible system; the lower system of the cable truss system is a free-form shell composed of rigid members while the upper system passes through the roof. The upper and lower system form an equivalent thickness space bearing system

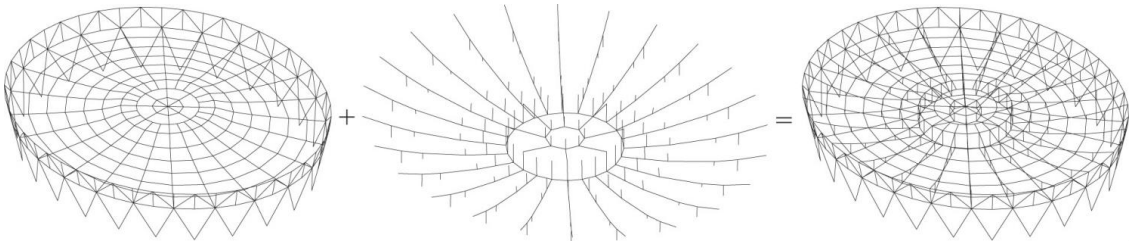

Fig. 1 The Yueqing Gymnasium

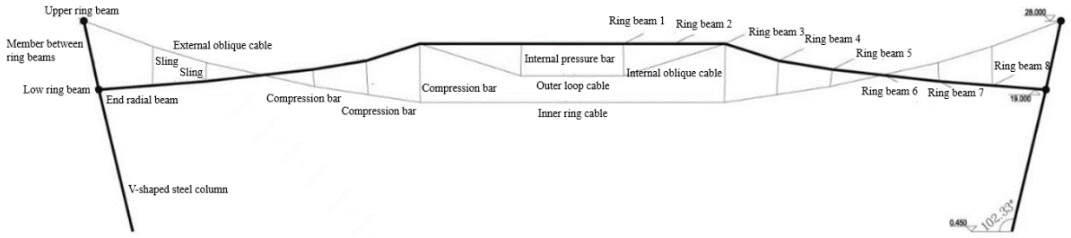

Fig. 2 Short-axis profile view of the roof structure of Yueqing Gymnasium (thick line is the rigid system, thin line is the flexible system)

through the sling, compression bar and ring cables, the main force cable system includes radial inclined cables, compression bars and ring cables, but the upper and lower system are connected by slings and compression bars and only the innermost ring compression bars are connected to the ring cables. This configuration offers the characteristics of the cable truss system and is a new hybrid space structure system (as shown in Fig. 2).

Pre-tension is a key factor to ensure structural safety, especially as the structure system of Yueqing Gymnasium is novel, the span is large, and it is located in a typhoon-prone area. Thus, it is essential to obtain the pre-tension changes over the service life of the structure with the help of long-term real-time cable monitoring technology, to further quantitatively evaluate the safety performance of the structure from the cable monitoring results. At the beginning of the construction of the project, it was decided to use the magnetic flux cable force measurement method to monitor the structure during the whole construction process.

3. Working principles of magnetic flux sensors

Magnetic flux sensors are based on the principle of magnetic elastic effect of ferromagnetic materials. That is, when the external mechanical stress σ borne by the ferromagnetic material changes, the internal magnetization (permeability) μ changes. The mathematical model of the relationship between the permeability change $\Delta\mu$ and the stress σ of ferromagnetic materials is shown as formula (1) (Wang *et al*.2005).

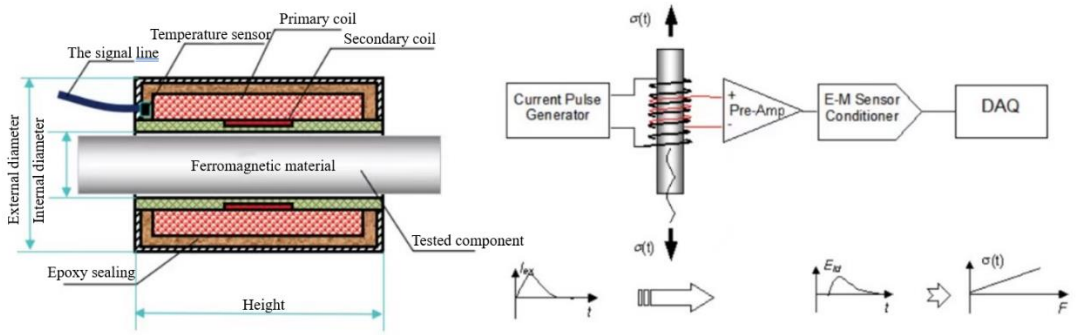

Fig. 3 Basic structure diagram and measurement principle of a magnetic flux sensor

$$\Delta\mu = -2\lambda_m \left(\frac{\mu_1}{B_m}\right)^2 \sigma \tag{1}$$

where, λ_m is the magneto-elongation coefficient of the ferromagnetic material in the magnetization saturation state, μ_1 is the magnetic permeability of the ferromagnetic material without external force, and B_m is the magnetic induction intensity in the magnetization saturation state.

The structural diagram of the magnetic flux sensor is shown in Fig. 3 (Huang *et al*. 2021), which consists of primary and secondary coils. If an AC excitation signal is applied to both ends of the primary coil, an alternating magnetic field that changes with time will be generated, and according to Faraday's law of electromagnetic induction, an induced electromotive force will be generated in the secondary coil (Wang *et al*. 2000, Wang *et al.* 2001)

$$V_{ind(t)} = -N\frac{d\emptyset}{dt} \tag{2}$$

The magnetic flux through the coil is along the direction of the tested object. During the test, the test piece may not be completely filled with the coil, so the total magnetic flux is composed of two parts: the magnetic flux passing through the air and the magnetic flux passing through the test piece. The induced voltage is shown in formula (3).

$$-N\frac{d\emptyset}{dt}\left[\mu_0 \int_{S_{\mu_0}} H(\rho,\varphi,t)ds + \int_{S_\mu} B(\rho,\varphi,t)ds\right] \tag{3}$$

Among them, S_{μ_0} and S_μ are the cross-sectional areas of the coils occupied by air and specimen, respectively. μ_0 is the magnetic permeability of air. If the induced voltage is integrated over time, the resulting output voltage V_{out} averaged over time Δt is shown in formula (4).

$$V_{out} = -\frac{1}{\Delta t}\int_{t_1}^{t_2} V(t)_{ind}\,dt = \frac{N}{\Delta t}\frac{d\emptyset}{dt}\left[\mu_0 \int_{S_{\mu_0}} \Delta H(\rho,\varphi,t)ds + \int_{S_\mu} \Delta B(\rho,\varphi,t)ds\right] \tag{4}$$

Among them, ΔH and ΔB are the changes of magnetic field strength and magnetic flux density in the time interval $t_2 - t_1$ respectively, and at the same time the current increases from 0 to I_a, and the corresponding magnetic field strength of I_a is H_a. The permeability to be measured is the magnetic permeability when the magnetic field strength is H_a. If the coil has a large number of turns and is closely arranged, the magnetic field within it will be almost uniform, even if there is an

iron core. Therefore the formula (4) can be simplified as

$$V_{out} = \frac{N}{\Delta t}\left[\mu_0(S_0 - S_f)\Delta H + S_f \Delta B\right] \tag{5}$$

where, S_0 is the cross-sectional area of the secondary coil of the sensor, which is related to the size of the sensor; S_f is the net cross-sectional area of the monitoring cable body, which is related to the size of the measuring member; When no test piece is placed in the coil, the integral of the output voltage changing with time is

$$V_0 = \frac{N}{\Delta t}\mu_0 S_0 \Delta H \tag{6}$$

From Eqs. (5) and (6) we can get

$$\mu = \frac{\Delta B}{\Delta H} = \mu_0\left[1 + \frac{S_0}{S_f}\left(\frac{V_{out}}{V_0} - 1\right)\right] \tag{7}$$

Therefore, the calculation formula of relative magnetic permeability μ_r is (Wang *et al.* 2005)

$$\mu_s(f,T) = 1 + \frac{S_0}{S_f}\left(\frac{V_{out}}{V_0} - 1\right) \tag{8}$$

where, $\mu_s(f,T)$ is the relative magnetic permeability (ratio of magnetic permeability to vacuum magnetic permeability) when cable force is *f* and temperature is T;

The magnetic permeability of steel changes with temperature, which affects the measurement results, therefore the temperature effect needs to be eliminated during measurement. At normal temperatures (-30℃~60℃), the slope of the relationship between the component's permeability and stress does not change with temperature. Therefore, in practical applications, the current measured values are usually calibrated to a unified temperature scale, which is called standard temperature T_0 here, as shown in formula (9).

$$\mu_s(f,T_0) = \mu_s(f,T) - \alpha(T - T_0) \tag{9}$$

where $\mu_s(f,T_0)$ is the relative magnetic permeability when cable force is f and temperature is T_0 and T_0 is usually taken as 20℃; α is the temperature compensation coefficient (provided by the factory).

For the ferromagnetic material cable structure, several sets of tests were carried out in the laboratory Tests under force and temperature to establish the relative permeability change and structure After determining the relationship between stress and temperature, it can be used to measure the cable member internal force.

For the cable structure of ferromagnetic material, if several sets of tests under different stress and temperature are carried out in the laboratory, then the relationship between the relative magnetic permeability change μ_r and the structural stress and temperature can be established, which can be used to measure the internal force of the cable member.

The relationship between the relative magnetic permeability change, μ_r , and the internal force, *f*, of the component can usually be expressed by the *n*th order polynomial equation, and the linear or cubic polynomial is usually used for fitting

$$f = c_0 + c_1\mu_r \tag{10}$$

$$f = c_0 + c_1\mu_r + c_2{\mu_r}^2 + c_3{\mu_r}^3 \tag{11}$$

where, μ_r is the relative magnetic permeability increment (the difference between the relative

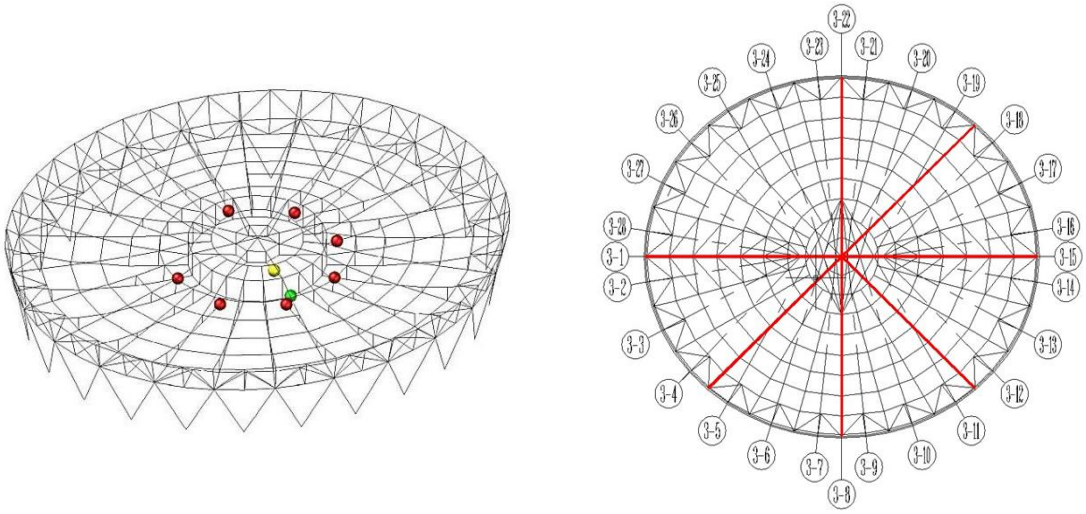

(a) Three-dimensional schematic diagram

(b) Schematic diagram of plane axis where the magnetic flux sensors are located

Fig. 4 Schematic diagram of sensor locations in Yueqing Gymnasium

magnetic permeability when the cable force is f after temperature correction and the relative magnetic permeability when the cable force is zero); $c_0 \sim c_3$ are the coefficients of the $f - \mu_r$ fitting curve.

4. Cable force monitoring scheme using magnetic flux method in Yueqing Gymnasium

Using a magnetic flux sensor is a common method for cable tension monitoring. Due to the different cable types, sizes and other parameters, the relationship between magnetic permeability and cable force of different cables varies, so they should be calibrated individually before leaving the factory to get the zero point of magnetic flux. The relationship between the magnetic permeability and cable force of each cable also needs to be calibrated and then the practical engineering application can be carried out. In particular, the feasibility and accuracy of the application of the magnetic flux method in the large-diameter non-closed Galfan cable used in Yueqing Gymnasium needs to be studied, and the effect of its application over the whole construction process in monitoring the new long-span cable-truss string-supported structure system is worth discussing. Therefore, according to the key nodes of cable force measurement, this paper divides the work into two stages: calibration stage, and tensioning construction stage.

4.1 Measuring position

Ten key representative measuring positions were determined based on the technical requirements for the health monitoring of Yueqing Gymnasium, in combination with the analysis of the stress characteristics of the steel structure during the construction and service period. The layout of these

Table 1 The locations and numbers of magnetic flux sensors in gymnasium

Sensor number	Monitoring object	The axis location
1#	Outer radial cable	3-4\5
2#	Outer radial cable	3-11\12
3#	Outer radial cable	3-22
4#	Outer radial cable	3-18\19
5#	Outer radial cable	3-8
6#	Outer ring cable	3-8\9
7#	Outer radial cable	3-1
8#	Outer ring cable	3-9\10
9#	Outer radial cable	3-15
10#	Inner radial cable	—

Fig. 5 PS-500 data acquisition instrument (magnetoelastic instrument)

measuring points is shown in Fig. 4. Fig. 4(a) is the three-dimensional schematic diagram of the measuring points for the steel cable forces where the red balls represent the positions of the outer radial cable sensors, the green ball shows the position of the outer ring cable sensors, and the yellow ball is the location of the inner radial cable sensor. Fig. 4(b) shows the axis numbers of the magnetic flux sensors. Table 1 shows the location and number of the magnetic flux sensors in the gymnasium.

4.2 System composition

The monitoring system is composed of a PS-500 magnetoelastic instrument, magnetic flux sensors of different specifications developed and produced by Liuzhou OVM Co., Ltd. and acquisition software (as shown in Figs. 5 and 6).

4.3 Cable and sensor parameters

A total of ten Galfan cables with three diameters were monitored, including seven external radial cables, two outer ring cables and one inner radial cable. The cable body and sensor parameters are

Fig. 6 Large diameter magnetic flux sensors

Table 2 Cable body and sensor specifications

Serial number	Cable type	Number	Cable diameter (mm)	Cable cross-sectional area (mm^2)	Sensor Type	Sensor cross-sectional area (mm^2)
1	Outer radial cable	7	110	7232	CCT120J	13273
2	Outer ring cable	2	135	10510	CCT145J	17970
3	Inner radial cable	1	38	883.6	CCT43B	1734

shown in Table 2, where CCT120J means that the sensor diameter is 120 mm, which is generally 5-10 mm larger than the cable diameter.

5. Study on influencing factors of cable force monitoring by magnetic flux method for large diameter non-closed Galfan cable

5.1 Test conditions

This test was completed in Hebei Juli Rigging Co., Ltd. Before the formal tests, over-tensioning was carried out to eliminate the residual stress of the cable body. The over-tensioning of the upper and lower radial cables and the inner ring cables are carried out in the tension groove equipped with a 2000t tensioning testing machine. During the over-tensioning process, before the cables leave the factory, we carried out a series of test studies while calibrating the relative magnetic permeability-cable force correlation.

5.2 Test methods

In the formal tensioning process, to accurately fit the correlation between the relative magnetic

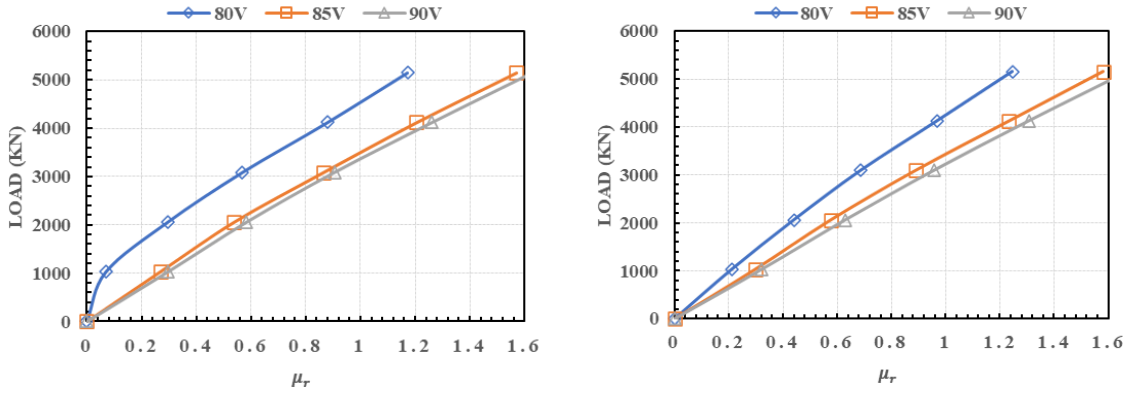

(a) 2 m away from the cable head (b) 13 m away from the cable head

Fig. 7 Comparison of calibration results of different charging and discharging voltages

permeability and the cable force, the over-tensioning process is divided into 10 levels of loading, and each level is maintained for 10 minutes. In the process of data analysis and data fitting, the method of a controlling single variable is used to study the regularity of the relationship between cable tension and magnetic permeability under the conditions of diffrerent charging and discharging voltages, different positions and different cable lengths, and to analyze the influence of relevant factors on the accuracy of cable tension monitoring.

The accuracy of the magnetic flux sensor is greatly affected by temperature, so it is necessary to measure the temperature of the sensors and then correct the relationship of cable force-relative permerbility according to formula (2), that is uniformly correcting to the 20℃ temperature scale. Since the test is carried out at room temperature, the temperature is constant at about 5℃ during the calibration test stage. The above test parameters will not be explained one by one in subsequent test studies.

5.3 Study on the influence of charging voltage

The magnitude of the charging voltage applied to the primary coil of the magnetic flux sensing system determines whether the cable can be fully magnetized, thus directly determining the test accuracy. Generally, the larger the diameter of the cable, the greater the charging voltage required. However, long-term use of excessive charging voltage will also cause unnecessary loss to the device. In order to study the suitable charging voltage for large diameter Galfan cable, firstly, the cables corresponding to the sensor CCT120J-121201D are loaded and tensioned when the sensor is placed 2 m and 13 m away from the cable head, and the charging voltages are 80V, 85V and 90 V, respectively. The results are shown in Fig. 7.

Fig. 7 shows that when the sensor is placed 2 m and 13 m away from the cable end, the charging voltage of 80 V is quite different from that of 85 V and 90 V, and the linearity is poor. When the charging voltage is set to 85 V or 90 V, the vacuum integral voltage is very close, and the calibration curve shows a very good linear relationship.

Therefore, it is concluded that the charging voltage should be set at least above 85 V for this large diameter cable. The subsequent comparative tests were carried out under charge and discharge voltages of 85 V or 90 V according to diameter changes.

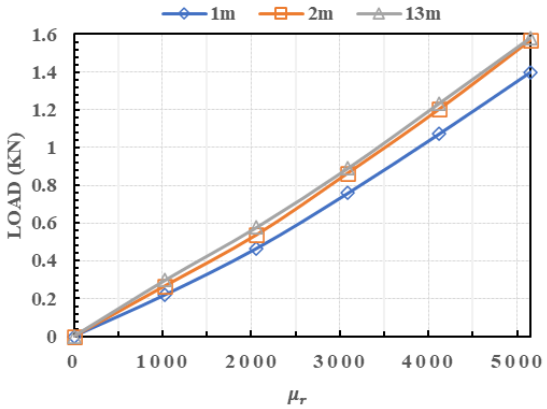

Fig. 8 Influence of sensor installation position

5.4 Study on the influence of sensor location

Theoretically, the cable are uniform when the cable is not stressed. However, due to the influence of the chemical composition, internal organizational structure, cross-section size of the cable and the twist of the steel wire, the measured integral values at different positions of the cable are different. That is, the relationship of cable force to relative magnetic permeability increment is the same, but the measurement value of V_0 is different. Therefore, the sensor should be kept at the same position during the monitoring. Considering that the force at the end of cable is relatively complex, the relationship between cable force and magnetic permeability is easily affected by other factors. Therefore, it is hoped that the sensor is installed at a certain distance from the end of cable. However, if it is too far away, installation at height will be difficult. Therefore, it is hoped to choose an installation location that is convenient for installation but with same rules with that at the middle span such as 13 m location. In the Yueqing Gymnasium project, the furthest distance for workers to reach from the cable end at height is about 2 m. Therefore, we selected the 2 m and 13 m positions in order to analyze the difference in measurement rules. In order to analyze the working rules at different distances from the root within 2 m, we chose a position of 1m away from the cable end. The test results are shown in Fig. 8.

It can be seen from Fig. 8 that the cable force-relative permeability increment relationship measured by the sensor installed at 1m from the cable head has more obvious nonlinear characteristics, and there is a large gap compared to the measured values of the sensors at 2 m and 13 m from the cable head. This is mainly because the 1 m position is close to the cable head, so the stress conditions are complex, which is not conducive to the calibration of the cable force. However, the linearity of the test results is already very good when it is laid at 2 m, and the difference compared to the measured value of the sensor at 13 m is very small (the small difference is caused by the gravity), that is, the test accuracy can be satisfied at 2 m away from the cable head, and this position is also within the distance range that is convenient for construction and installation. It is required to strictly confirm the calibration position of the sensor on the cable, and install it at the same position during on-site measurement. In addition, experience shows that the installation position of the sensor on the cable should be careful to avoid cable clamps, tensioning fixtures, etc.

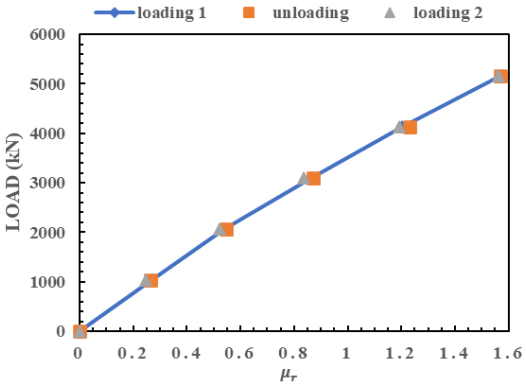

(a) $f-\mu_r$ when the charging votage is 85 V

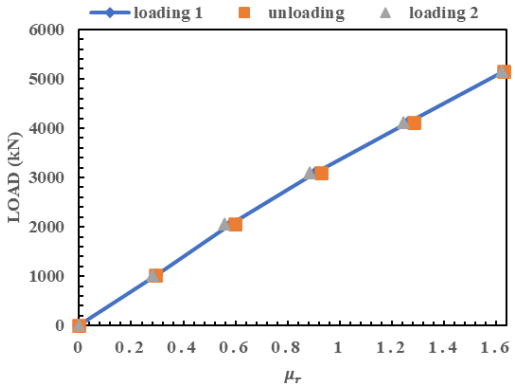

(b) $f-\mu_r$ when the charging votage is 90 V

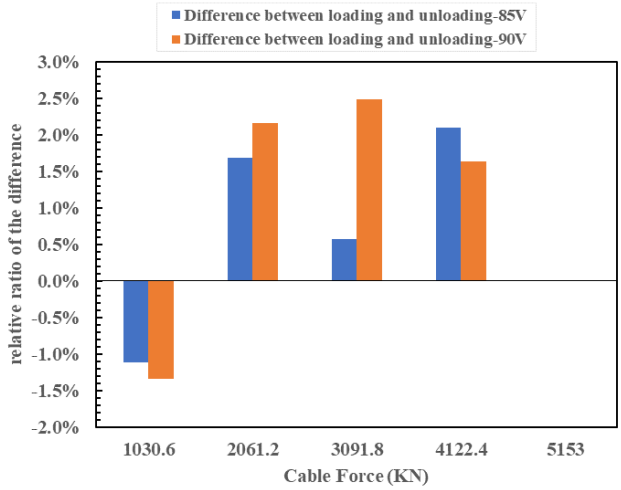

(c) relative ratio of the maximum difference between loading and unloading

Fig. 9 Loading and unloading reciprocating test results (D=110 mm)

5.5 Study on the reliability of the method

The actual cable body will experience the loading and unloading reciprocating process during the construction tensioning process. To study the reliability when the method was applied to such large diameter Galfan cables, the loading-unloading-reloading cyclic tests were carried out on the cables with 110 mm and 135 mm diameter, respectively.

5.5.1 The reliability of the method for the cable with D=110 mm

For the Galfan cables with a diameter of 110 mm, we carried out loading-unloading-reloading cyclic tests at charging voltages of 85 V and 90 V, respectively. The test results in Figs. 9(a) and 9(b) show that for the Galfan cable with 110 mm diameter, the reciprocating curves of the loading and unloading process are almost coincident with good linearity. From Fig. 9(c)， it can be seen that when the charging votage is 85 V, the maximium relative difference between the loading and unloading processes is less 2% at the same load level ; and when the working votage is 90 V, the

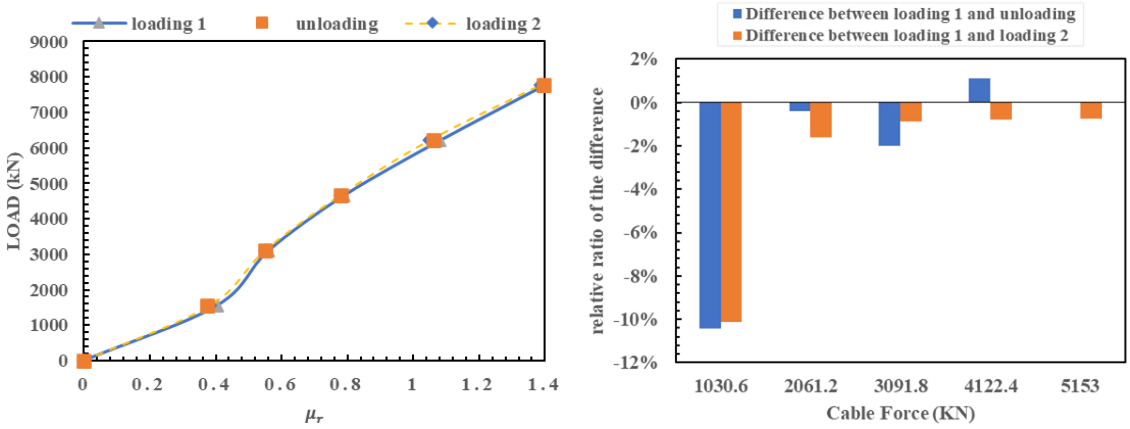

(a) $f-\mu_r$ during the loading and unloading process

(b) relative ratio of the maximum difference between loading and unloading

Fig. 10 Loading and unloading reciprocating test results (D=135 mm)

maximum relative difference between the loading and unloading processes is 2.49%. There are no apparent difference on two groups of tests. The above analysis verifies the reliability of the method.

5.5.2 The reliability of the method for the cable with D=135 mm

For the Galfan cables with a diameter of 135 mm, we carried out loading-unloading-reloading cyclic tests at charging voltages of 90 V according to the previous conclusion on the influence of charging voltages. The test results in Figs. 10(a) and 10(b) show that for the Galfan cable with 135 mm diameter, the reciprocating curves of the loading and unloading process are in good agreement when the load exceeds 20% of the ultimate load, with about 2% maximum difference. However, in the low stress stage, obvious nonlinearity is displayed, and the difference in measured values during the loading and unloading process reaches 10%. This is due to the low stress stage, which causes a small change in the total magnetic permeability, so the relative error increases. But for the Yueqing Gymnasium project, the design cable strength of the hoop cables is above 3000 KN. For most actual projects, the design value of cable force under normal use is generally between 20-30%. Therefore, it can be concluded that the magnetic flux method is suitable for monitoring 135 mm diameter Galfan cable under a certain stress level.

5.6 Study on the $f-\mu_r$ fitting curve of Galfan cables with diameter greater than 100 mm

In order to study the relationship between cable force and relative magnetic permeability increment when magnetic flux sensors are applied to cables with diameters greater than 100 mm, the comparative experiments are conducted on seven radial cables (D=110 mm) and two ring cables (D=135 mm). The research results are shown in Figs. 11 and 12. It can be seen from Fig. 11 that when the cable diameter is 110mm, the cable force-relative magnetic permeability increment of the seven cables has a relatively good linear correlation, and the linear fitting degree is between 0.9951 and 0.997. After cubic polynomial fitting, the fitting degree has been further improved. It can be seen from Fig. 12 that the linear fitting degree of the ring cable with a diameter of 135 mm is low,

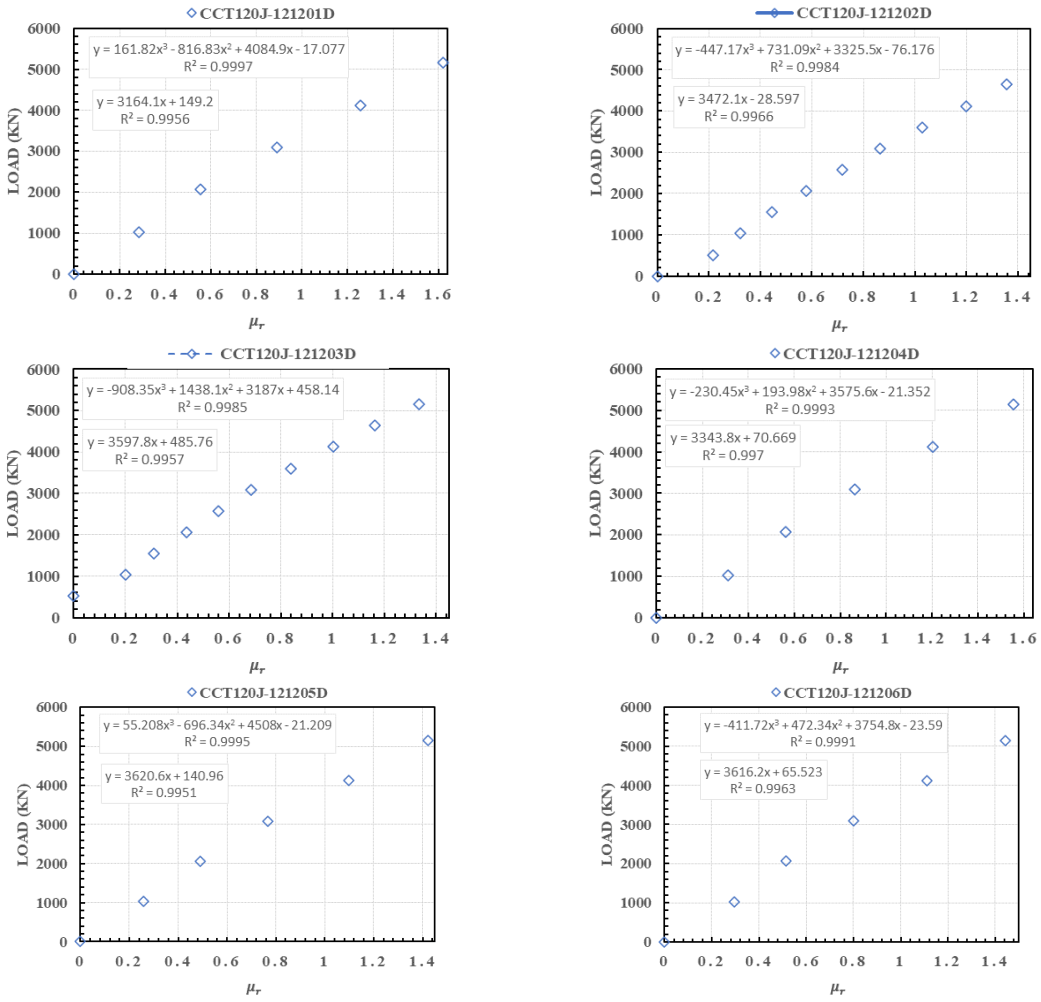

(a) the $f-\mu_r$ fitting curves of cables with 100mm diamer

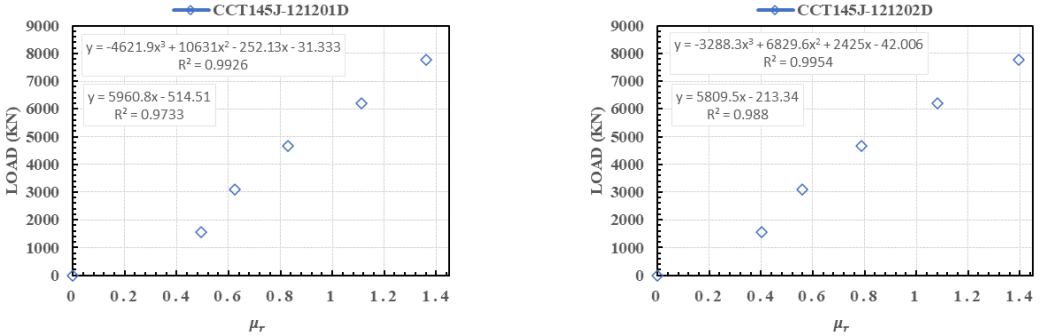

(b) the $f-\mu_r$ fitting curves of cables with 135mm diamer

Fig. 11 the $f-\mu_r$ fitting curves of cables with diamer greater than 100 mm

Fig. 12 System composition diagram

only 97.26%. When cubic fitting is used, the fitting degree is significantly improved, reaching more than 99%. From this, it can be concluded that for cables with diameters below 110 mm, in order to improve on-site measurement efficiency, linear fitting can be used to determine the $\boldsymbol{f-\mu_r}$ correlation. However, in order to improve monitoring accuracy, it is appropriate to use cubic or above polynomials to calibrate the $\boldsymbol{f-\mu_r}$ relationship. For larger diameter cables (such as 135 mm), the $\boldsymbol{f-\mu_r}$ must be calibrated with a cubic or above polynomial.

6. Cable force monitoring in tensioning construction stage

6.1 Monitoring scheme

After the calibration test in the cable factory, the magnetic flux sensors are permanently installed on the cable body and transported to the site for installation. After the overall tensioning, the pre-tension of the cable body is applied and formed for normal service. In this process, whether the pre-tension reaches the expected value is particularly important. The Yueqing Gymnasium project has established a cable tension monitoring system based on the magnetic flux method to monitor the cable tension in the whole process of construction. In this process, the magnetic flux sensors on the cables are connected to the data aquisition machine PS-500 through a 16-channel switch box, and the sensor adopts a 24-hour timing sampling scheme, and intensive collection is carried out after the completion of every step of the tensioning operation. In order to ensure the test accuracy, for each cable force measurement, the system automatically samples three times and then takes the average integral voltage value to calculate the relative permeability in the actual tensioning state, and then calculates the cable force according to the cable force-relative permeability curve obtained in the calibration stage.

6.2 Monitoring results

The cable force monitoring results of the latter two stages of tensioning were compared with the limited pressure gauge data on site, and the results are shown in Fig. 13.

Note: The sub-figures in Figs. 13(f) and 13(h) without a measured oil pressure gauge value mean that the cable is not actively tensioned in the tensioning stage and is passively tensioned, so there is no oil pressure gauge value at the step. This shows that cable force monitoring is an important supplementary method for real-time monitoring of cable force changes in the construction process.

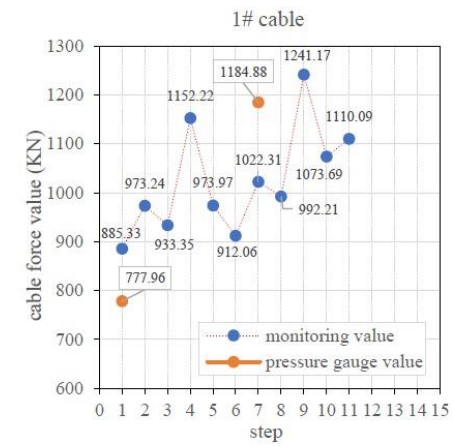

(a) Cable #1

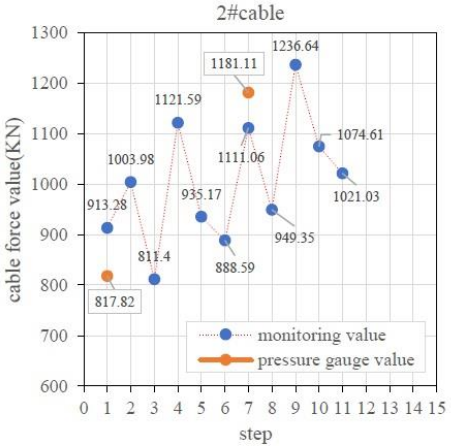

(b) Cable #2

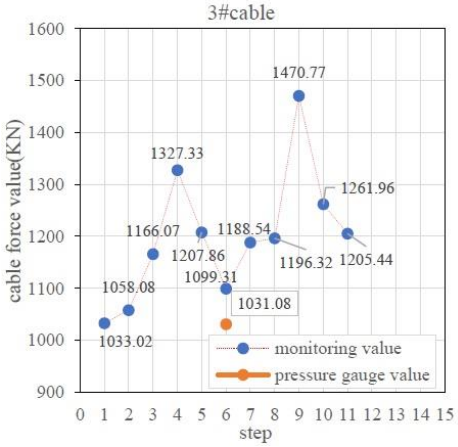

(c) Cable #3

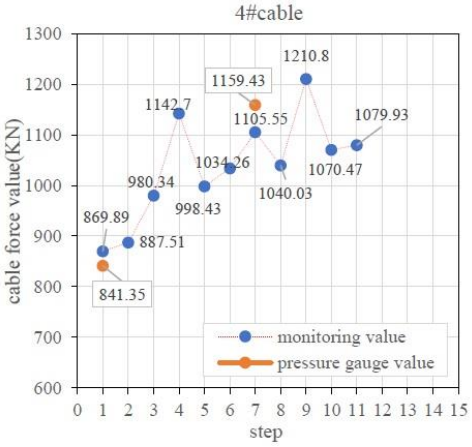

(d) Cable #4

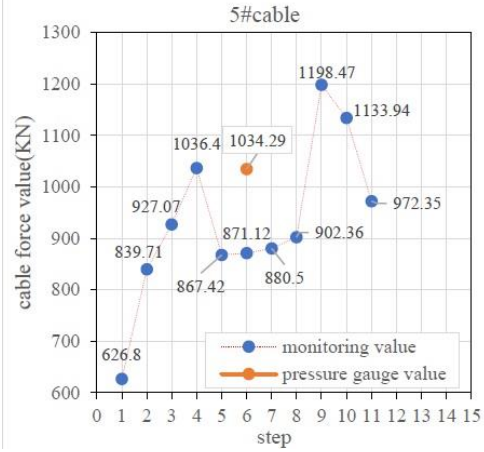

(e) Cable #5

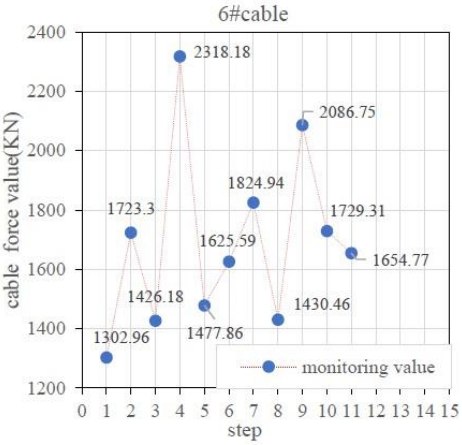

(f) Cable #6

Fig. 13 Cable numbers 1-9: Cable monitoring value vs Pressure gauge value

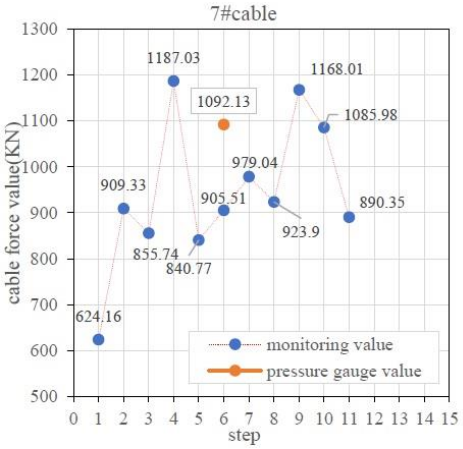

(g) Cable #7

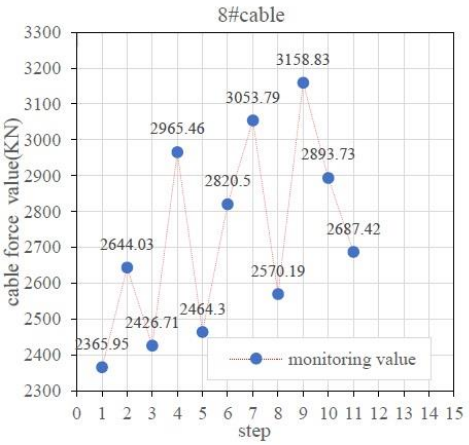

(h) Cable #8

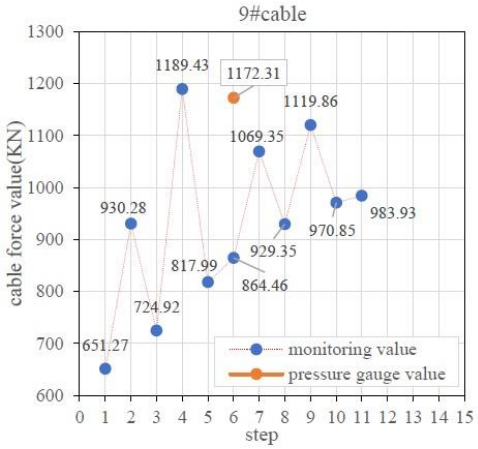

(i) Cable #9

Fig. 13 Continued-

As shown in Fig. 13, by comparing the measured value of cable force, monitored by the magnetic flux sensor, with the oil pressure gauge value, the minimum error between the two values is 2.65%, while on average it is ~8%. Only the error of an individual measuring points is larger than 10%. After analyzing the oil pressure gauge value, it was found to be unstable at that measuring moment, and there was a big difference between several recorded values. Additionally, the oil pressure gauge value represents the force applied at the end of the cable but there is a gap between the installation position of the magnetic flux sensor and the end. Also, the cable body turn over and the additional effect of other cable bodies will cause some variation, so there may be a deviation between the actual cable force obtained in the cable body and the cable force value measured by the oil pressure gauge, but the overall pre-stress change trend is consistent.

It can also be seen from Fig.13 that with the development of the tensioning construction, due to the complex effect of loading and unloading among the cable system components, the local cable force increases or decreases. From the analysis of the overall data trends, the data fluctuates around an obvious ascending line, indicating that each cable segment gradually obtains pre-tension. After

tensioning, the final cable force reaches the design pre-tension value.

Comparison between the monitoring value and the oil pressure gauge value shows that the application of the magnetic flux method can provide a feasible basis for real-time monitoring of the structural tensioning process of a cable-truss string-support system.

7. Conclusions

This paper studies the application of magnetic flux sensors in the monitoring of Galfan cable tension based on the Chinese Yueqing Gymnasium, which is the largest span cable-truss string-support structure in the world. The main conclusions and discussions are as follows.

(1) The magnetic flux sensor method is applied to the cable force measurement of large-diameter unsealed high-vanadium smooth cables. The loading and unloading process has high linearity and high repeatability, and the method is feasible.

(2) For Galfan cables with large diameter above 100mm, the charging and discharging voltage should be above 85V.

(3) If the sensor is placed very close to the cable head, the relationship of cable force-relative permeability shows enhancing nonlinear property. However, it is not convenient for installation if it is too far away from the cable head. A distance of 2m from the cable head is recommended for it can meet both the test accuracy requirements and the availability for installation.

(4) During the calibration test phase of the cable factory, shorter cables can be used instead of actual cables for calibration.

(5) By comparing the cable force monitoring results, using the magnetic flux sensor at the end of tensioning, with the design tensioning force, the relative error between the actual pre-tension of most cables and the design value is within 10%. The cable force value fluctuates but rises slowly during the tensioning process.

It can be concluded that the magnetic flux method is an effective way to provide supplementary information to understand the actual cable force development. In the follow-up work, we will conduct in-depth research on the identification accuracy of magnetic flux method in the cable force monitoring of larger diameter Galfan cables and the impact of severe temperature changes in combination with actual projects. The method in this paper can provide a useful reference for cable force monitoring of Galfan cables based on magnetic flux method.

Compliance with ethical standards

Funding: The first author was partially sponsored by the National Natural Science Foundation of China (No. 50808125), Shanghai Science and Technology Development Funds (No. 08QA14054).
Conflict of Interest: The authors declare that they have no conflict of interest.

Acknowledgments

The calibration test work in this paper was carried out in China Juli rigging Co., Ltd. and we sincerely thank Juli rigging Co., Ltd. for its strong support.

References

Acampora, A., Macdonald, J.H.G., Georgakis, C.T. and Nikitas, N. (2014), "Identification of aeroelastic forces and static drag coefficients of a twin cable bridge stay from full-scale ambient vibration measurements", *J. Wind Eng. Ind. Aerod*., **124**, 90-98. https://doi.org/10.1016/j.jweia.2013.10.009.

Azim, M.R., Zhang, H. and Gui, M. (2020), "Damage detection of railway bridges using operational vibration data: theory and experimental verifications", *Struct. Monit. Maint*., **7**(2), 149-166. https://doi.org/10.12989/smm.2020.7.2.149.

Barnard, N.C. and Brown, S.G.R. (2008), "Modelling the relationship between microstructure of Galfan-type coated steel and cut-edge corrosion resistance incorporating diffusion of multiple species", *Corrosion Sci*., **50**(10), 2846-2857. https://doi.org/10.1016/j.corsci.2008.07.005.

Camassa, D., Castellano, A., Fraddosio, A., Miglionico, G. and Piccioni, M.D. (2021), "Dynamic identification of tensile force in tie-rods by interferometric radar measurements", *Appl. Sci*., **11**(8), 3687. https://doi.org/10.3390/app11083687.

Coarita, E. and Flores, L. (2015), "Nonlinear analysis of structures cable – truss", *Int. J. Eng. Technol*., **7**(3).

Dong, Z., Fan, P., Li, P. Mao. Y. (2020), "Experimental study on the sensitive parameters of nondestructive test method for the cable based on the leakage magnetic principle", *Proceedings of the 2nd International Conference on Environmental Prevention and Pollution Control Technologies(EPPCT2020)*, **474**, 1877-1884. https://doi.org/10.26914/c.cnkihy.2020.055545.

Furukawa, A., Suzuki, S. and Kobayashi, R. (2022), "Tension estimation method for cable with damper using natural frequencies and two-point mode shapes with uncertain modal order", *Front. Built Environ*., **8**. https://doi.org/10.3389/fbuil.2022.906871.

Gaute Alonso, A., Garcia Sanchez, D., Alonso Cobo, C. and Calderon Uriszar Aldaca, I. (2022), "Temporary cable force monitoring techniques during bridge construction-phase: The Tajo River Viaduct experience", *Scientific Reports*, **12**, 7689. https://doi.org/10.1038/s41598-022-11746-z.

Geuzaine, M., Foti, F. and Denoël, V. (2021), "Minimal requirements for the vibration-based identification of the axial force, the bending stiffness and the flexural boundary conditions in cables", *J. Sound Vib*., **511**. https://doi.org/10.1016/j.jsv.2021.116326.

Han, S.E. and Koh, H.S. (2008), "Dynamic behavior characteristics of the open-shaped hybrid dome Structural system subjected to wind loads", *J. Architect. Inst. Korea Struct. Constr*., **24**(8), 131-138.

Huang, H., Yin, C. and Wang, X. "Application of magnetic flux sensor in cable force monitoring of closed high vanadium cable", *Sci. Technol. Innov. Herald*, **18**(16), 24-27, (In Chinese).

Huynh, T.C. and Kim, J.T. (2014), "Impedance-based cable force monitoring in tendon-anchorage using portable PZT-interface technique", *Math. Probl. Eng*., https://doi.org/10.1155/2014/784731.

Jakiel, P. and Mańko, Z. (2017), "Estimation of cables' tension of cable-stayed footbridge using measured natural frequencies", *MATEC Web of Conferences*, **107**, 00006. https://doi.org/10.1051/matecconf/201710700006.

Kernicky, T., Whelan, M. and Al-Shaer, E. (2018), "Dynamic identification of axial force and boundary restraints in tie rods and cables with uncertainty quantification using Set Inversion Via Interval Analysis", *J. Sound Vib*., **423**, 401-420. https://doi.org/10.1016/j.jsv.2018.02.062.

Kim, B.H. and Park, T. (2007), "Estimation of cable tension force using the frequency-based system identification method", *J. Sound Vib*., **304**(3-5), 660-676. https://doi.org/10.1016/j.jsv.2007.03.012.

Kim, J.T., Huynh, T.C. and Lee, S.Y. (2014), "Wireless structural health monitoring of stay cables under two consecutive typhoons", *Struct. Monit. Maint*., **1**(1), 47-67. https://doi.org/10.12989/smm.2014.1.1.047.

Kim, S.W., Jeon, B.G., Kim, N.S. and Park, J.C. (2013), "Vision-based monitoring system for evaluating cable tensile forces on a cable-stayed bridge", *Struct. Health Monit*., **12**(5-6). https://doi.org/10.1177/1475921713500513.

Lai, G.G., Yang, C. and Su, C.T. (2010), "Estimation and management of magnetic flux density produced by underground cables in multiple-circuit feeders", *Eur. T. Electrical Power*, **20**(5), 545.558. https://doi.org/10.1002/etep.333.

Lai, G.G., Yang, C.F. and Su, C.T. (2010), "Estimation and management of magnetic flux density produced by underground cables in multiple-circuit feeders", *Eur. T. Elec. Power*, **20**(5), 545-558. https://doi.org/10.1002/etep.333.

Li, Z., Zhang, Z. and Dong, S. (2015), "Introduction to the design of the long-span space rope truss architecture of Yueqing Sports Center Stadium", *Spatial Struct.*, **21**(4), 38-44. https://doi.org/10.13849/j.issn.1006-6578.2015.04.038.

Li, Z., Zhang, Z. and Yu, W. (2017), "Design and analysis of cord truss string structure of Yueqing Sports Center Gymnasium", *Struture*, **47**(11), 82-86. https://doi.org/10.19701/j.jzjg.2017.11.014.

Liu, H., Guo, L., Chen, Z., Meng, Y. and Zhang, Y. 2021), "Study on bonding mechanism of hot-cast anchorage of Galfan-coated steel cables", *Eng. Struct*., **246**, 112980. https://doi.org/10.1016/j.engstruct.2021.112980.

Liu, L., Li, C., Li., R. and Feng. H. (2017), "An extended Preisach model for effects of magnetization history on magnetomechanical behavior of steel cables", *Smart Struct. Mater. + Nondestructive Eval. Health Monit.*, https://doi.org/10.1117/12.2258361.

Mike, J.C. (2012), "Fifty years of progress for shell and spatial structures", *Proceedings of the Institution of Civil Engineers - Engineering History and Heritage*, **2**. https://doi.org/10.1680/ehah.12.00003.

Morgenthal, G., Rau, S., Taraben, J. and Abbas, T. (2018), "Determination of stay-cable forces using highly mobile vibration measurement devices", *J. Bridge Eng*., **23**(2). https://doi.org/10.1061/(ASCE)BE.1943-5592.0001166.

Park, S., Kim, J.W., Lee, C. and Lee, J.J. (2014), "Magnetic flux leakage sensing-based steel cable NDE technique", *Shock Vib*., https://doi.org/10.1155/2014/929341.

Park, S., Kim, J.W., Lee, C., Lee, J. and Gil, H.B. (2012), "Local fault detection technique for steel cable using multi-channel magnetic flux leakage sensor", *J. Comput. Struct. Eng. Inst. Korea*, **25**(4), 287-292. https://doi.org/10.7734/COSEIK.2012.25.4.287.

Park, S.H., Kim, J.W., Nam, M.J. and Lee, J.J. (2012), "Magnetic flux leakage sensing-based steel cable NDE technique incorporated on a cable climbing robot for bridge structures", *Adv. Sci. Technol*., **83**, 217-222. https://doi.org/10.4028/www.scientific.net/AST.83.217.

Ren, L., Xiu, C., Li, H., Lu, Y., Wang, J. and Yao, X. (2018), "Development of elasto-magnetic (EM) sensor for monitoring cable tension using an innovative ratio measurement method", *Smart Mater. Struct*., **27**. https://doi.org/10.1088/1361-665X/aae0b0.

Schröppel, W. (2014), "Bauen mit Leichtigkeit – Ein spannendes Montagekonzept", *Stahlbau*, **83**(6), 406-411. https://doi.org/10.1002/stab.201410165.

Sun, G., Li, X. and Wu, J. (2020), "Postfire mechanical properties of Galfan-coated steel cables", *Fire Mater*., **44**(7), 909-922. https://doi.org/10.1002/fam.2892.

Sun, G., Li, X., Xue, S. and Chen, R. (2019), "Mechanical properties of Galfan-coated steel cables at elevated temperatures", *J. Constr. Steel Res*., **155**, 331-341. https://doi.org/10.1016/j.jcsr.2019.01.002.

Sun, G., Xiao, S. and Qu, X. (2021), "Thermal–mechanical deformation of Galfan-coated steel strands at elevated temperatures", *J. Constr. Steel Res*., **180**. https://doi.org/10.1016/j.jcsr.2021.106574.

Wang, M.L., Chen, Z.L. and Koontz, S.S. (2000), "Magnetoelastic method of stress monitoring in Steel Tendons and Cables", Nondestruct. Eval. Highways，Utilities, Pipelines IV., P roceedings of SPIE.

Wang, M.L., Lloyd, G. and Hovorka, O. (2001), "Development of a remote coil magneto—elastic stress sensor for steel cables", *Proceedings of the SPIE 8th Annual International Symposium on Smart Structures and Material, Health Monitoring and Management of Civil Infrastructure Systems*, New port Beach CA.

Wang, S., Chen, Z., Liu, H. and Yu, Y. (2018), "Experimental study on stress relaxation properties of structural cables", *Constr. Build. Mater*., **175**, 777-789. https://doi.org/10.1016/j.conbuildmat.2018.04.224.

Wang, S., Wang, W., Su, Y., *et al*. "Magnetic model of the relationship between relative permeability change and stress of ferromagnetic materials", *J. Xi'an Univ. Sci. Technol.*, **25**(3), (In Chinese).

Xiong, E., Wang, S. and Miao, X. (2012), "Research on magnetomechanical coupling effect of Q235 steel member specimens", *J. Shanghai Jiaotong Univ.* (*Science*), **17**, 605-612. https://doi.org/10.1007/s12204-012-1332-7.

Yishu, Z., Jinning, Z., Liu, C. and Cao, J. (2019), "Performance analysis of by-pass excitation cable force

sensor", *IOP Conference Series: Mater. Sci. Eng*., **647**, 012017. https://doi.org/10.1088/1757-899x/647/1/012017.
Yishu, Z., Ping, A., Jinjin, C., Jinning, Z. and Chang, L. (2019). "Design of by-pass excitation cable force sensor", *J. Phys.: Conference Series*. https://doi.org/10.1088/1742-6596/1267/1/012068.
Yu, Z., Shao, S., Liu, N., Zhou, Z., Feng, L., Du, P. and Tang, J. (2021), "Cable tension identification based on near field radiated acoustic pressure signal", *Measurement*, **178**. https://doi.org/10.1016/j.measurement.2021.109354.
Yuan, J. and Wu, S. (2011), "Experimental study on stress-magnetic effect of cable", *Proceedings of SPIE 2011 International Conference on Photonics, 3D-Imaging, and Visualization*, 313-317.
Zhang, S.C., Xu, X.M., Gao, F., Luo, B., Shi, W.Z. and Fang, Q. (2022), "Experimental study on corrosion of galfan-coated full-locked coil ropes in a natatorium environment", *Adv. Civil Eng*., **2022**, https://doi.org/10.1155/2022/9777836.
Zhang, Z., Ding, J. and Zhang, Y. (2014), "Research on the structural composition of annular truss and its engineering application", *J. Build. Struct*., **35**(4), 11-19. https://doi.org/10.14006/j.jzjgxb.2014.04.004.
Zurru, M. (2021), "Non-linear normal modes of plane cable trusses", *Comput. Struct*., **257**, https://doi.org/10.1016/j.compstruc.2021.106662.

JK